Journal of Solid State Chemistry 183 (2010) 1340–1346

Contents lists available at ScienceDirect

Journal of Solid State Chemistry

journal homepage: www.elsevier.com/locate/jssc

One-dimensional CoPt nanorods and their anomalous IR optical properties

X.W. Zhou [a,*], R.H. Zhang [a], D.M. Zeng [b], S.G. Sun [b,**]

[a] College of Chemistry and Life Science, Three Gorges University, Yichang 443002, People's Republic of China
[b] State Key Laboratory of Physical Chemistry of Solid Surfaces, Department of Chemistry, College of Chemistry and Chemical Engineering, Xiamen University, Xiamen 361005, People's Republic of China

ARTICLE INFO

Article history:
Received 29 September 2009
Received in revised form
23 February 2010
Accepted 4 April 2010
Available online 9 April 2010

Keywords:
CoPt nanorods
In situ FTIRs
Abnormal infrared effects

ABSTRACT

One-dimensional (1D) CoPt nanorods were synthesized by a galvanic displacement reaction. The morphology of the nanomaterials was characterized by transmission electron microscopy (TEM), scanning electron microscopy (SEM) and X-ray powder diffraction (XRD). Energy-dispersive X-ray spectroscopy (EDS) analysis confirmed the coexistence of Co and Pt in the 1D nanorods. Studies of cyclic voltammetry (CV) demonstrated that the 1D CoPt nanorods exhibit a better electrocatalytic property for CO oxidation than that of bulk Pt electrode does. *In situ* electrochemical FTIRS illustrated, for the first time, that the 1D CoPt nanorods display abnormal infrared effects (AIREs), which was previously revealed mainly on 2D film nanomaterials.

1. Introduction

Nanostructured CoPt materials possess novel optical, electrical, catalytic and magnetic properties, which depend strongly on the size and shape of the nanoparticles. A number of CoPt nanomaterials of different morphologies such as spheres [1,2], nanowires [3–5], nanonods [6], nanoclusters [7], and core-shell structure [8,9] have been prepared by different methods. Among them, the template approach was usually employed to synthesize one-dimensional (1D) CoPt nanowires [10,11]. One shortage of the template method consists in the common procedure of the removal of template, which may destroy the structure of the products and limit their applications. Galvanic displacement reaction is a special template method, in which one substance is served as a suitable sacrificial template and reacts with other appropriate metal ions according to their different standard reduction potentials, resulting in the formation of excellent hollow particles that take on the shape of the sacrificial template. This method was used widely to obtain hollow metal nanostructures of various shapes [12–19]. Vasquez et al. [19] have reported one-pot synthesis of hollow CoPt nanospheres using Co nanoparticles as the sacrificial templates.

It has been revealed that nanometer scale thin film materials of platinum group metals and their alloys exhibit anomalous IR properties, in which the adsorbed molecules on these nanomaterials may yield anomalous IR features, named the surface enhanced IR absorption (SEIRA) [20,21], the Fano-like resonance (Fano-like) [22–24] and the abnormal IR effects (AIREs) [25,26]. Further investigations showed that nanostructured Ni and Co thin films also display anomalous IR properties [27–29]. It has demonstrated that the anomalous IR features significantly depended on the size, structure, and agglomeration states of nanoparticles [30–32]. It is worthwhile pointing out that all previous studies concerning the anomalous IR properties were carried out mainly with nanomaterials of films (two-dimensional (2D) structure) and of assembly of nanoparticles (three-dimensional (3D) nanostructure). It is also important to note that the study of anomalous IR properties of nanomaterials with different morphologies is of great interests in revealing the fundamentals of nanomaterials [33].

In this paper, 1D CoPt nanorods were synthesized and characterized, and IR optical properties of the nanomaterials were investigated. The study revealed that the 1D CoPt nanorods exhibit abnormal infrared effects (AIREs).

2. Experimental

2.1. Synthesis of 1D CoPt nanorods

In a typical synthesis procedure, the 1D CoPt nanorods were synthesized using the galvanic displacement reaction. In brief, 0.1 mL of 0.4 M $CoCl_2$ solution was added to 50 mL ultrapure H_2O solution containing 100 mg poly(vinylpyrrolidone) (PVP). Then, 25 mL of 0.01 M freshly prepared $NaBH_4$ solution was added dropwise with stirring. Once the $NaBH_4$ is completely dropped

* Corresponding author. Fax.: +86 0592 2180181.
** Corresponding author.
E-mail addresses: xwzhou@ctgu.edu.cn (X.W. Zhou), sgsun@xmu.edu.cn (S.G. Sun).

0022-4596/$ - see front matter © 2010 Elsevier Inc. All rights reserved.
doi:10.1016/j.jssc.2010.04.003

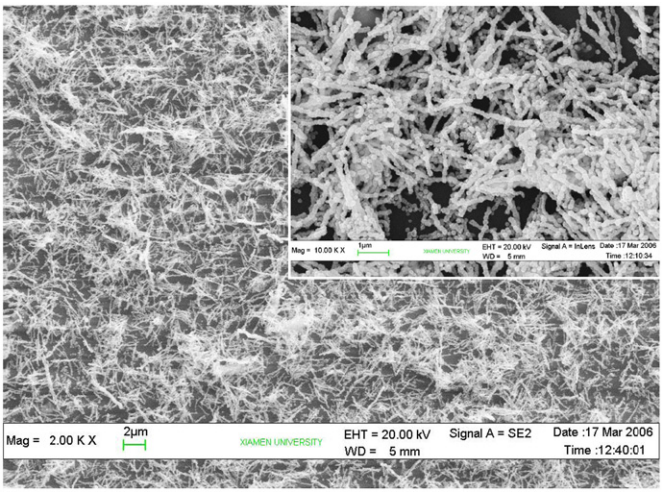

Fig. 1. Low and high-magnification SEM images of 1D CoPt nanorods.

into solution, 20 mL of 0.4 M K_2PtCl_6 was added dropwise. To avoid oxidation of the Co nanoparticles, high-purity N_2 was bubbled into the solution throughout the whole process. The obtained dark gray colloidal solution was separated, washed thoroughly, and then redispersed into Millipore H_2O for ultimate studies.

2.2. Characterization and preparation of electrodes

Scanning electron microscopy (SEM) images were acquired on LEO-1530 electron microscopy. High-resolution transmission electron microscopy (HRTEM) patterns were obtained on instruments of FEI Tecnai-F30 electron microscopy. The powder samples were characterized by powder X-ray diffration (XRD) using a Panalytical X'pert PRO diffractormeter.

A prescribed quantity of suspension of CoPt nanorods was applied to the surface of glassy carbon (GC) or bulk Au electrode, upon which a drop of 0.5% (V/V) Nafion solution was dispersed to fix the nanomaterials on the surface. The electrode thus prepared is denoted thereafter as CoPt/GC or CoPt/Au. The cyclic

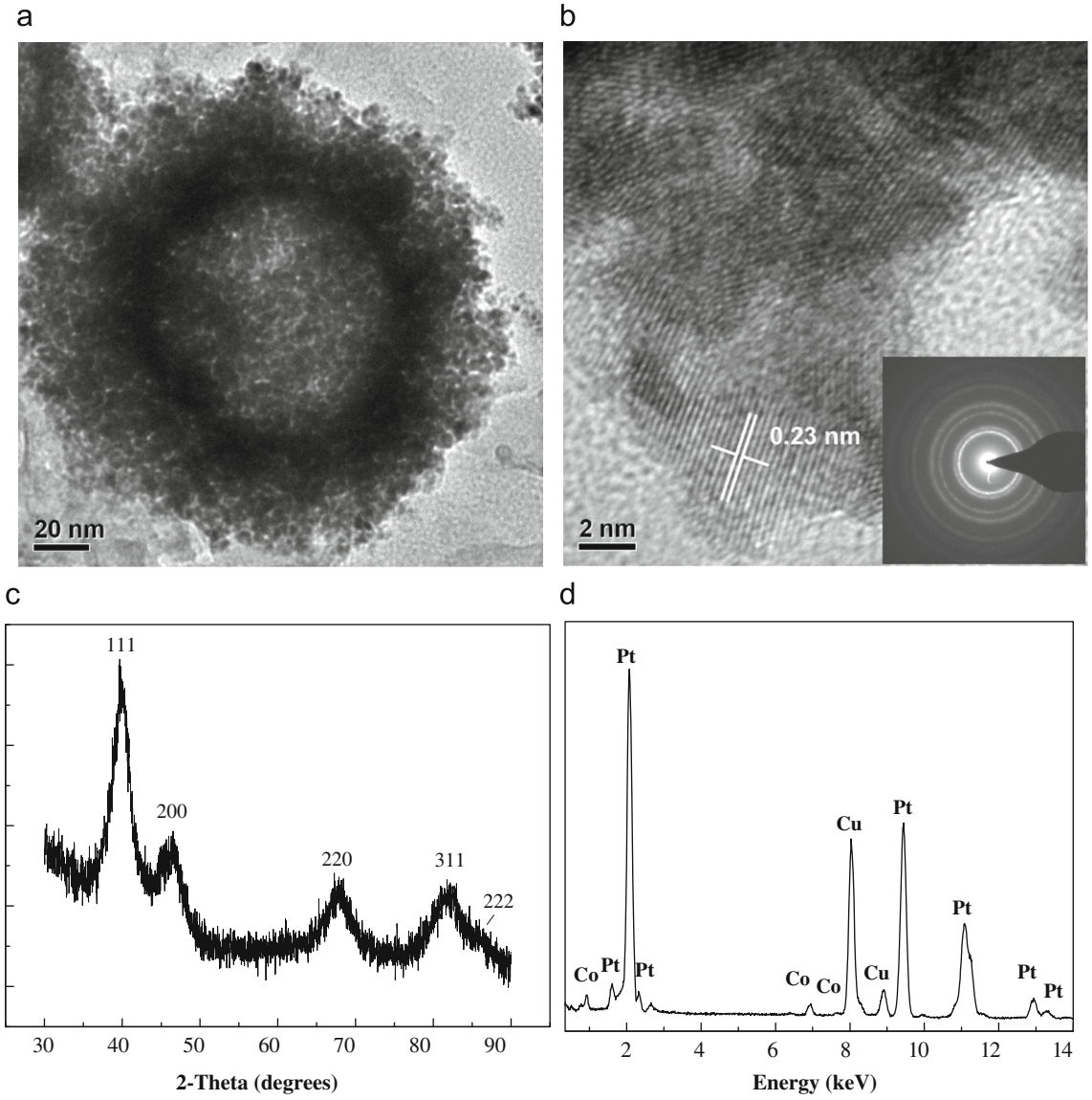

Fig. 2. (a) TEM, (b) high-resolution TEM images, (c) XRD patterns, and (d) EDS spectra of the 1D CoPt nanorods. The inset to (b) shows a selected area electron diffraction.

voltammetric studies were carried out on a CHI 631C electrochemical work station (CH instruments, Inc.), at a potential scan rate 50 mV · s^{-1}.

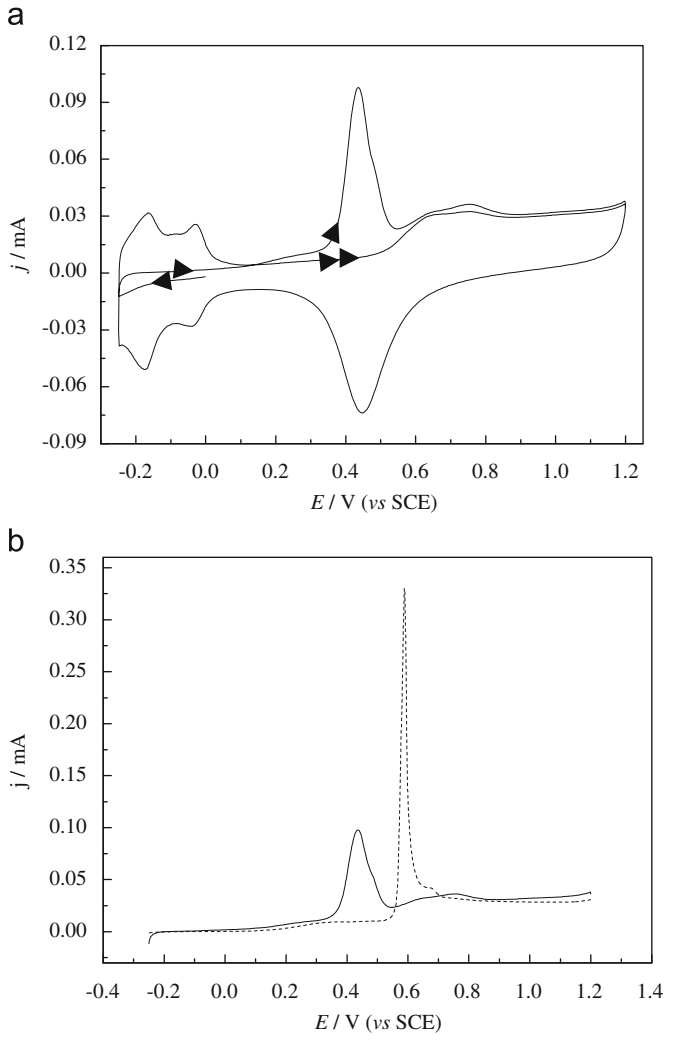

Fig. 3. (a) Cyclic voltammograms of oxidation of adsorbed CO on CoPt/GC, (b) Comparison of adsorbed CO oxidation on CoPt/GC (solid line), on bulk Pt (dash line) in 0.1 M H_2SO_4, sweep rate 50 mV · s^{-1}

2.3. Electrochemical in situ FTIR spectroscopy

Electrochemical *in situ* FTIR spectroscopic measurements were carried out on a Nexus 870 FTIR spectrometer (Nicolet) equipped with an EverGlo IR source and a liquid nitrogen-cooled MCT-A detector. The MSFTIRs (multi-step FTIR spectroscopy) [34] and SPAFTIRs (single potential-alteration FTIR spectroscopy) [35] procedures were used in the present study. In the MSFTIRs experiments, a series of single-beam spectra were collected first at sample potentials (E_S), where adsorbed CO is stable, and a single-beam spectrum was collected finally at the reference potential (E_R), at which adsorbed CO has been removed completely by electrooxidation. In the SPAFTIRs experiments, at both $E_{s'}$ and E_R, adsorbed CO can adsorb stably on the electrodes as demonstrated directly by CV studies. The resulting spectra were calculated using the following formulas,

$$\frac{\Delta R}{R} = \frac{R(E_S) - R(E_R)}{R(E_R)} \quad (1)$$

where $R(E_S)$ and $R(E_R)$ are single-beam spectra of reflection collected at sample potential E_S and reference potential E_R, respectively. Each single-beam spectrum was recorded by collecting and co-adding 400 interferograms at a spectral resolution of 8 cm^{-1}.

3. Results and discussion

3.1. Characterization of 1D CoPt nanorods

Low and high-magnification SEM images in Fig. 1 illustrate that large-scale 1D CoPt nanorods have been synthesized. It can be seen that the nanomaterials are composed of some distorted nanosphere chains. The average diameter of the nanospheres is measured about 200 nm. The high-magnification TEM image reveals the detail structure of the nanomaterials. Fig. 2a displays one nanosphere, from which we can see that the surface of the nanosphere is composed of small particles. Fig. 2b is a high-resolution TEM (HRTEM) image taken from the surface of an individual CoPt nanosphere. The lattice-spacing value is measured at 0.23 nm, which matches well with the lattice of {1 1 1} plane of platinum metal, indicating that the shell surface of the CoPt nanosphere may consist of small Pt nanocrystals. The selected area electron diffraction (SAED) pattern inserted to Fig. 2b

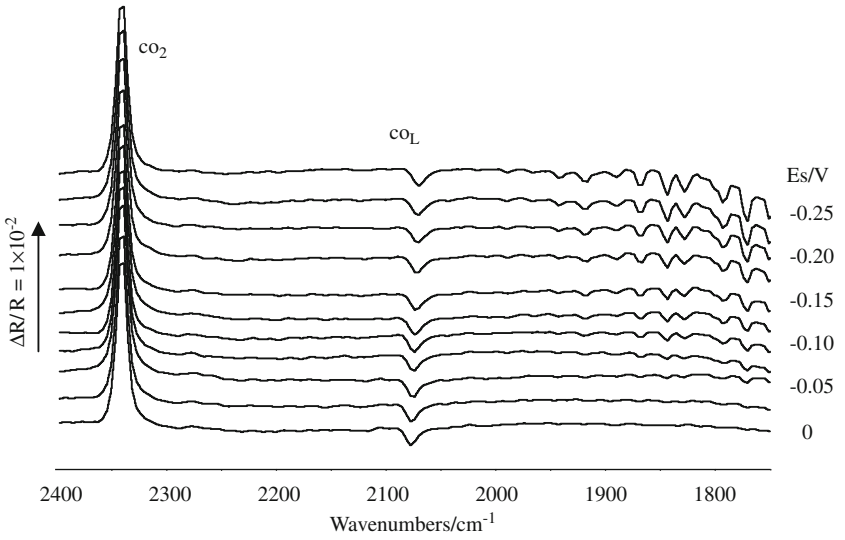

Fig. 4. *In situ* MSFTIR spectra of CO adsorbed on bulk Pt electrodes in 0.1 M H_2SO_4, E_R=1.0 V, $E_{s'}$ is indicated for each spectrum.

illustrates a chemically disordered face-centered cubic (fcc) polycrystalline structure. The concentric rings can be assigned as {1 1 1}, {2 0 0}, {2 2 0} and so on.

The powder XRD results also confirmed such a structure. Compared to the pure Pt nanoparticles, the diffraction angles of the CoPt nanorods were shifted to the higher positions, reflecting the lattice contraction due to partial substitution of Pt by Co [36,37]. As shown in Fig. 2c, however, the peak position of the (1 1 1) diffraction does not shift toward to a high angle, suggesting that the surface of the 1D CoPt nanorods was mostly composed of Pt nanocrystals. The energy-dispersive X-ray spectroscopy (EDS) data (Fig. 2d) demonstrate that the CoPt nanosphere chains present an average stoichiometry of Co_8Pt_{92}.

3.2. Electrocatalytic properties of 1D CoPt nanorods for co oxidation

Fig. 3a illustrates cyclic voltammograms of oxidation of adsorbed CO on the CoPt/GC electrode in 0.1 M H_2SO_4. It can be seen that the hydrogen adsorption-desorption current is completely suppressed when the electrode surface was covered with CO. The onset potential of CO oxidation is measured at about 0.10 V, and the main oxidation current peak appears around 0.44 V. In the second cycle, well-known CV features of a Pt polycrystalline electrode are observed. Two distinct pairs of current peaks around −0.03 and −0.17 V are typical characteristics of hydrogen adsorption-desorption on Pt surface. The formation of Pt oxide is occurred in potentials above 0.65 V in the positive-going potential scan, for which oxidation current is observed clearly. In the reverse scan, a reduction current peak of Pt oxide is recorded at 0.45 V. It is worthwhile to note that the onset potential of CO oxidation on a bulk polycrystalline Pt is 0.15 V and the current peak locates around 0.58 V under the same

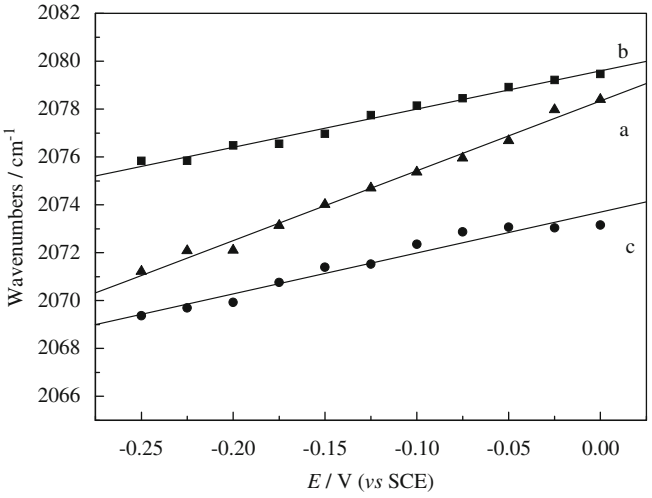

Fig. 6. Plots of CO_L band centre versus E for CO adsorbed on (a) bulk Pt, (b) CoPt/GC, and (c) CoPt/Au electrodes.

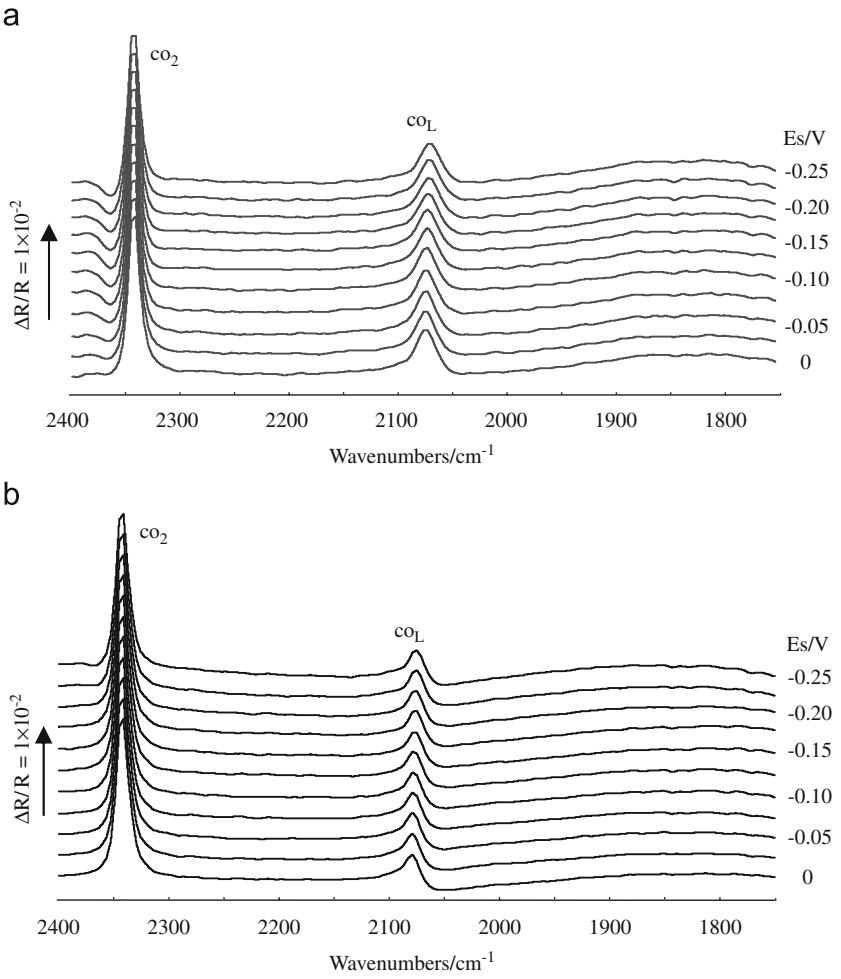

Fig. 5. *In situ* MSFTIR spectra of CO adsorbed on (a) CoPt/GC and (b) CoPt/Au electrodes in 0.1 M H_2SO_4, E_R=1.0 V, E_s is indicated for each spectrum.

conditions (Fig. 3b). These results demonstrated that the 1D CoPt nanorods exhibit better electrocatalytic properties for CO oxidation than that of bulk Pt does in 0.1 M H_2SO_4.

3.3. Anomalous IR properties of 1D CoPt nanorods

3.3.1. Results of MSFTIRs

The IR optical properties of the 1D CoPt nanorods and a bulk Pt electrode were studied by using CO as a probe molecule. Fig. 4 shows the MSFTIR spectra for CO adsorbed on the bulk Pt electrode in 0.1 M H_2SO_4. The negative-going band around 2072 cm^{-1} is assigned to IR absorption of linearly bonded CO (CO_L) at $E_{s'}$ that is varied from $-0.25 \sim 0$ V. The center of this band is shifted positively with increasing $E_{s'}$, yielding a Stark tuning rate of 29.2 cm^{-1} V^{-1} (Fig. 6a) [38]. The value of the Stark tuning rate is closely correlated with the concentration of electrolyte [31,39,40] and solution molecule [41]. Except for the band of CO_L, a positive-going band located near 2341 cm^{-1} is ascribed to IR absorption of CO_2 species that are uniquely derived from the oxidation of CO_{ad} at E_R, because no CO_2 and CO species presented initially in solution inside the thin layer between the electrode and IR window. The most CO_2 species can be retained in the thin layer due to a large resistance of diffusion, which has been confirmed by our previous work [20–24]. It is necessary to note that the IR band of CO_{ad} on a bulk Pt electrode always appears in the opposite direction to the CO_2 band under the present MSFTIRs experimental conditions, which is in accordance with the predication of Eq (1).

Fig. 5a shows the MSFTIR spectra of CO adsorbed on the CoPt/GC electrode in 0.1 M H_2SO_4 under the same conditions. It can observe clearly that the IR features are different from those of CO_{ad} on the bulk Pt electrode consisting in the following respects.

Table 1.
Variation of parameters of the CO_L band on different electrodes.

	CoPt/GC	CoPt/Au	Bulk Pt
FWHM (cm^{-1})	20	15	12
Stark tuning rate ($cm^{-1}V^{-1}$)	17.1	16.0	29.2
Δ_{IR}	4.2	3.1	1

(1) The IR band of the CO_L is slightly blue-shifted (from 2072–2077 cm^{-1}), and most importantly the direction of the CO_L band is inverted completely, signifying an anomalous IR absorption. As a consequence, the CO_L band is appeared in the same direction as that of the CO_2 band.

(2) The intensity of the CO_L band is increased. As mentioned previously, the integral intensity of the CO_2 band can be used as a measure of the quantity of CO_{ad}, thus, the enhancement factor (Δ_{IR}) defined as the ratio of the normalized CO_{ad} IR band intensity on the CoPt/GC electrode versus that on the bulk Pt electrode surface, i.e.,

$$\Delta_{IR} = \frac{(A^{CO_L}_{CoPt}/A^{CO_2}_{CoPt})_{CoPt/GC}}{(A^{CO_L}_{Pt}/A^{CO_2}_{Pt})_{BulkPt}} \quad (2)$$

where $A^{CO_L}_{CoPt}$ and $A^{CO_2}_{CoPt}$ refer to integral intensities of the CO_L and CO_2 bands, respectively, measured in IR spectra of CoPt/GC electrode; $A^{CO_L}_{Pt}$ and $A^{CO_2}_{Pt}$ are the integral intensities of the CO_L and CO_2 bands acquired in the IR spectra of the bulk Pt electrode. From Eq (2), the Δ_{IR} is evaluated at 4.2 that indicates an enhancement of 4.2 times of IR absorption of CO_L on the CoPt/GC electrode.

(3) The IR absorpti/on of CO_L band of CoPt/GC electrode is broadened. The full width at half-maximum (FWHM) of the CO_L band in spectra recorded on CoPt/GC electrode is measured about 20 cm^{-1}, which is 8 cm^{-1} broader than that measured in the spectra acquired on the bulk Pt electrode (12 cm^{-1}) under the same conditions.

These anomalous phenomena are the typical IR features of abnormal infrared effects (AIREs) that are observed initially for CO adsorbed on nanostructured thin films (2D nanomaterials) of platinum metals and alloys [24,30]. The above results demonstrated clearly that CO adsorbed on the 1D CoPt nanorods yields the AIREs, which is the first time to reveal the AIREs on the 1D nanomaterials.

It is known that the reflectivity of substrate may influence on IR optical features [42]. Glassy carbon (GC) is a moderately reflecting substrate, while bulk Au electrode belongs to a high reflecting one. In order to investigate the influence of substrate on IR properties of the 1D CoPt nanorods, CO adsorbed on the CoPt/Au electrode is also studied. Fig. 5b shows the MS-FTIR spectra of CO adsorbed on the CoPt/Au electrode under the same conditions as above. It can be seen that the IR bands of CO_L and CO_2 in Fig. 5b

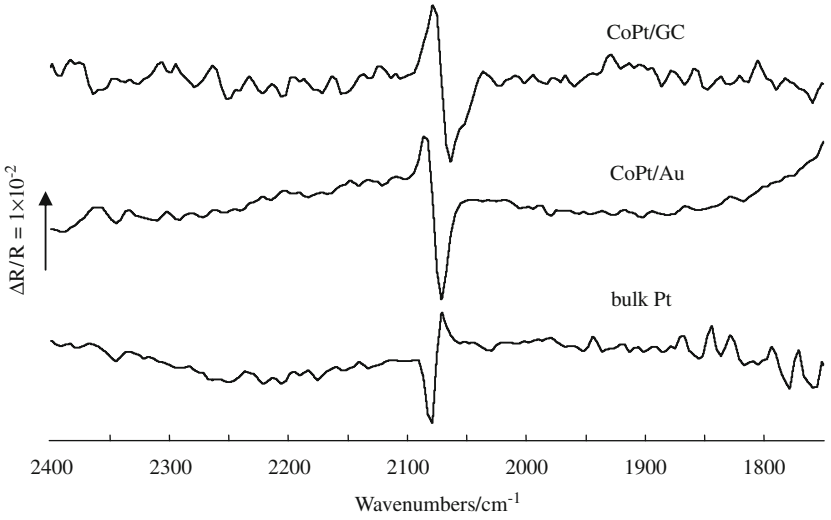

Fig. 7. *In situ* SNIFTIR spectra of CO adsorbed on CoPt/GC, CoPt/Au and bulk Pt electrodes in 0.1 M H_2SO_4, $E_R = -0.2$ V, $E_{s'} = 0$ V.

are appeared in the same direction as those seen in Fig. 5a, indicating clearly that the CoPt/Au electrode exhibits also the AIREs. The fact that both CoPt/GC and CoPt/Au produce the AIREs has confirmed that the anomalous IR features observed in Figs. 5a and b were generated mainly by the 1D CoPt nanorods, and that the influence of the substrate materials on the IR spectral features may be neglected in the present study. Actually, Weaver et al. [43] have observed that the IR absorption on the Pt nanoparticles (Pt/C) film on an Au substrate could be changed from normal absorption to anti-absorption. The detailed parameters of IR features of the CO_L band such as FWHM, Stark tuning rate and Δ_{IR} measured on the three kinds electrodes are compared in Table 1. The values of the FWHM, Stark tuning rate and Δ_{IR} obtained on the CoPt/Au electrode are 15 cm^{-1}, 16.0 cm^{-1} V^{-1} and 3.2, respectively, which are similar to those data measured on the CoPt/GC electrode.

3.3.2. Results of SPAFTIRs

The SPAFTIRs spectra of CO adsorbed on bulk Pt, CoPt/GC and CoPt/Au electrodes are displayed in Fig. 7. The $E_{s'}$ and E_R were set at 0 V and −0.2 V, respectively. The IR absorption of CO_{ad} in spectra collected by *in situ* SNIFTIRs produces will give rise to bipolar bands with their positive peak in low wavenumbers and negative peak in high wavenumbers due to Stark shift [38]. This is exactly the case of CO_L adsorbed on the bulk Pt electrode as shown in Fig. 7. The positive peak in the bipolar band is around 2070 cm^{-1} and the negative peak is around 2080 cm^{-1}. However, the IR features of CO adsorbed on CoPt/GC electrode is quite different from those of CO adsorbed on bulk Pt electrode. It is evident that the bipolar CO_L band in the spectra of CoPt/GC electrode is completely inverted, indicating an anomalous bipolar bands. Furthermore, the intensity of CO_L is enhanced. The anomalous bipolar band was first reported in 1994 in potential-difference FTIR spectra of a basal plane graphite disc covered with Pt particles [44]. They explained the anomalous bipolar CO band by a potential-induced migration of chemisorbed CO molecules from terraces at the reference potential to edge or kink sites at the sample potentials. It was assumed that the CO stretching is higher for terraces than for edge or kink sites. Later, Gutiérrez et al. [45] thought the explanation of the anomalous bipolar bands is simple and should be interpreted by the laws of reflectance, which mean that the moderately reflecting substrate (GC) was the origin of the anomalous shape of the bipolar bands. But, here we can obtain the same result when we use a high reflecting (bulk Au electrode) as the substrate (Fig. 7.). The IR features observed in the *in situ* SPAFTIRs studies are accordance with the results obtained in the above MSFTIRs investigations, which confirms again that the 1D CoPt nanorods yield AIREs.

The present results suggest that the optical phenomenon of the AIREs is mainly related to the 1D CoPt nanorods. In our previous work, we have reported that dispersed Pt, Pd nanoparticles and Pd nanoparticles confined in supercages of Y zeolites can yield EIRA while their agglomerates give the AIREs [20,31,46]. They thought the strong interaction between the nanoparticles and the collective interaction between CO adsorbate and the nanoparticles inside the agglomerates may be one of the origins of the AIREs. Here, we have stated above that the 1D CoPt nanorods were composed of some distorted nanosphere chains because of the magnetic interaction of Co nanoparticles. Actually, one 1D CoPt nanorod can be regarded as agglomerate, in which may exist collective interaction. Then we believe that the AIREs observed on the 1D CoPt nanorods belong to the structure of the nanomaterials. It is evident that to understand the origins of the AIREs, further studies involving not only experimental approaches but also theoretical analysis would be worthwhile.

4. Conclusions

In the current paper, one-dimensional CoPt nanorods were prepared through a galvanic displacement reaction. Cyclic voltammetric results demonstrated that the 1D CoPt nanorods display a better catalytic property than that of a bulk Pt for CO oxidation in 0.1 M H_2SO_4. It has been measured that the current peak potential of CO_{ad} oxidation on the CoPt/GC electrode is shifted negatively by 140 mV in comparison with the value measured on a bulk Pt electrode. The IR properties of the 1D CoPt nanorods were investigated by *in situ* FTIR reflection spectroscopy employing CO adsorption as probe reaction. It has revealed, for the first time, that the 1D CoPt nanorods present abnormal infrared effects (AIREs). The substrate materials do not affect significantly the anomalous IR features, as illustrated by the similar anomalous IR features observed for CO adsorbed on both CoPt/GC and CoPt/Au electrodes. The current study has extended effectively the investigation of abnormal infrared effects (AIREs), which were initially discovered on 2D film nanomaterials of platinum group metal and alloys, to 1D chain-like nanomaterials, and thrown a new insight into understanding the origin of the AIREs.

Acknowledgments

Financial supports from Natural Science Foundation of China (20828005, 20833005), the MOST (2009CB220102) and Scientific Research Funds for the Talents of Three Gorges University (KJ2009B003) are highly acknowledged.

References

[1] E.V. Shevchenko, D.V. Talapin, A.L. Rogach, A. Kornowski, M. Haase, H. Weller, J. Am. Chem. Soc. 124 (2002) 11480.
[2] V. Tzitzios, D. Niarchos, G. Margariti, J. Fidler, D. Petridis, Nanotechnology 16 (2005) 287.
[3] Y.H. Huang, H. Okumura, G.C. Hadjipanayis, J. Appl. Phys. 91 (2002) 6869.
[4] Z.T. Zhang, D.A. Blom, Z. Gai, J.R. Thompson, J. Shen, S. Dai, J. Am. Chem. Soc. 125 (2003) 7528.
[5] P. Beecher, E.V. Shevchenko, H. Weller, A.J. Quinn, G. Redmond, Adv. Mater. 17 (2005) 1080.
[6] V. Tzitzios, D. Niarchos, M. Gjoka, N. Boukos, D. Petridis, J. Am. Chem. Soc. 127 (2005) 13756.
[7] L.A. Hannour, B.B. Prével, P.E. Bernstein, M.A. Perez, J. Gierak, E. Bourhis, D. Mailly, Surf. Sci. 594 (2005) 1.
[8] J.I. Park, J. Cheon, J. Am. Chem. Soc. 123 (2001) 5743.
[9] C.H. Jun, Y.J. Park, Y.R. Yeon, J. Choi, W. Lee, S. Ko, J. Cheon, Chem. Commun. (2006) 1619.
[10] Y.K. Su, D.H. Qin, H.L. Zhang, H. Li, H.L. Li, Chem. Phys. Lett. 388 (2004) 406.
[11] J. Choi, S.T. Oh, H. Ju, J. Cheon, Nano lett. 5 (2005) 2179.
[12] Y. Sun, Y. Xia, Science 298 (2002) 2176.
[13] Y. Sun, B.T. Mayers, Y. Xia, Nano lett. 5 (2002) 481.
[14] Y. Sun, B.T. Mayers, Y. Xia, Adv. Mater. 15 (2003) 641.
[15] H.P. Liang, Y.G. Guo, H.M. Zhang, J.S. Hu, L.J. Wan, C.L. Bai, Chem. Commun. (2004) 1496.
[16] H.P. Liang, H.M. Zhang, J.S. Hu, Y.G. Guo, L.J. Wan, C.L. Bai, Angew. Chem. Int. Ed. 43 (2004) 1540.
[17] H.P. Liang, L.J. Wan, C.L. Bai, L. Jiang, J. Phys. Chem. B. 109 (2005) 7795.
[18] P.R. Selvakannan, M. Sastry, Chem. Commun. (2005) 1684.
[19] Y. Vasquez, A.K. Sra, R.E. Schaak, J. Am. Chem. Soc. 127 (2005) 12504.
[20] Y.X. Jiang, S.G. Sun, N. Ding, Chem. Phys. Lett. 344 (5-6) (2001) 463.
[21] A. Miki, M. Osawa, Chem. Commun. (2002) 1500.
[22] Y. Zhu, H. Uchida, M. Watanabe, Langmuir 15 (1999) 8757.
[23] A.E. Bjerke, P.R. Griffiths, W. Thess, Anal. Chem. 71 (1999) 1967.
[24] I. Tkach, A. Panchenko, T. Kaz, V. Gogel, K.A. Friedrich, E. Rodunner, Phys. Chem. Chem. Phys. 6 (2004) 5419.
[25] G.Q. Lu, S.G. Sun, S.P. Chen, Z.W. Tian, K.K. Shiu, Langmuir 16 (2000) 778.
[26] G. Orozco, C. Gutièrrez, J. Electroanal. Chem. 484 (2000) 64.
[27] H.C. Wang, S.G. Sun, J.W. Yan, H.Z. Yang, Z.Y. Zhou, J. Phys. Chem. B. 109 (2005) 4309.
[28] Q.S. Chen, S.G. Sun, J.W. Yan, J.T. Li, Z.Y. Zhou, Langmuir 22 (2006) 10575.
[29] O. Krauth, G. Fahsold, A. Pucci, J .Chem. Phys. 110 (1999) 3113.
[30] H. Gong, S.G. Sun, J.T. Li, Y.J. Chen, S.P. Chen, Electrochim. Acta 48 (2003) 2933.
[31] W. Chen, S.G. Sun, Z.Y. Zhou, S.P. Chen, J. Phys. Chem. B 107 (2003) 9808.
[32] Y.J. Chen, S.G. Sun, S.P. Chen, J.T. Li, H. Gong, Langmuir 20 (2004) 9920.

[33] C.X. Wu, H. Lin, Y.J. Chen, W.X. Li, S.G. Sun, J. Chem. Phys. 121 (2004) 1553.
[34] W.F. Lin, S.G. Sun, Electrochim. Acta 41 (1996) 803.
[35] D.S. Corrign, L.W.H. Legung, M.J. Weaver, Anal Chem 59 (1987) 2252.
[36] G. Chen, D. Xia, Z. Nie, Z. Wang, L. Wang, L. Zhang, J. Zhang, Chem. Mater. 19 (2007) 1840.
[37] A.R. Denton, N.W. Ashcroft, Phys. Rev. A 43 (1991) 3161.
[38] D.K. Lambert, Electrochim. Acta 41 (1996) 623.
[39] J.W. Russel, J. Overend, K. Scanlon, M. Severson, A. Bewick, J. Phys.Chem. 87 (1983) 293.
[40] K. Kunimatsu, H. Seki, W.G. Golden, J.G. Golden, M.R. Philpott, Surf. Sci. 158 (1985) 596.
[41] M.R. Anderson, D. Blackwood, T.G. Richmond, S. Pons, J. Electroanal. Chem. 256 (1988) 397.
[42] C. Pecharromán, A. Cuesta, C. Gutiérrez, J. Electroanal. Chem. 563 (2004) 91.
[43] S. Park, Y.Y. Tong, A. Wieckowski, M.J. Weaver, Electrochem. Commun. 3 (2001) 509.
[44] P.A. Christensen, A. Hamnett, J. Munk, G.L. Troughton, J. Electroanal. Chem. 370 (1994) 251.
[45] R. Oritiz, A. Cuesta, O.P. Márquez, J. Márquez, J.A. Mèndez, C. Gutièrrez, J. Electroanal. Chem. 465 (1999) 234.
[46] Y.X. Jiang, S.G. Sun, S.P. Chen, N. Ding, Chem. J. Chin. Univ. 11 (2001) 1860.